IOPscience iopscience.iop.org

Home Search Collections Journals About Contact us My IOPscience

Overhead line switching transients

This article has been downloaded from IOPscience. Please scroll down to see the full text article.

2002 J. Phys. A: Math. Gen. 35 7125

(http://iopscience.iop.org/0305-4470/35/33/310)

View the table of contents for this issue, or go to the journal homepage for more

Download details:
IP Address: 171.66.16.107
The article was downloaded on 02/06/2010 at 10:19

Please note that terms and conditions apply.

INSTITUTE OF PHYSICS PUBLISHING JOURNAL OF PHYSICS A: MATHEMATICAL AND GENERAL

J. Phys. A: Math. Gen. **35** (2002) 7125–7135 PII: S0305-4470(02)34565-7

Overhead line switching transients

A Maaouni[1] **and A Amri**

Laboratoire d'Electronique, d'Electromagnétisme et d'Hyperfréquences, Faculté des Sciences Aïn-Chock, Université HASSAN II, Casablanca, BP 5336 Maârif, Morocco

Received 5 March 2002, in final form 18 June 2002
Published 7 August 2002
Online at stacks.iop.org/JPhysA/35/7125

Abstract

An efficient method is presented for the determination of switching transients in overhead lines. This new approach is based on the partial fraction expansion of the network functions in the Laplace *s*-domain. Newton's algorithm is used to locate the poles in the complex *s*-plane. Accurate analytical expressions of the line parameters are used to take into account losses in the ground. Some simulation results are shown.

PACS numbers: 84.40.Az, 84.70.+p, 02.60.−x

1. Introduction

The determination of the overvoltage stresses in a power system network is of great importance for the design of overvoltage protection systems. In simulating switching transients, the most commonly employed transmission line models are distributed parameter models [1, 2]. Because the line parameters depend on the signal frequency [1], particularly when the ground return is involved, it is recommended to simulate in the frequency domain [3, 4]. The conventional approach is to use convolution techniques in conjunction with the Fourier transform to determine the impulse response of an arbitrary power-network system. While the explicit analytical expression of the impulse responses is impractical, the numerical inverse fast Fourier technique (FFT) suffers from the fact that a large number of frequency points is needed to avoid aliasing effects. The drawback of the direct convolution is that it is time consuming.

In this paper, an efficient and accurate frequency-dependent distributed parameter line model is used. This model was obtained directly from the scattering theory [5] under quasi-TEM hypothesis [6]. Recently, it has been proved that the transmission line characteristics, in this model, may be calculated analytically at less computational cost [7]. On the other hand, the impulse responses of the network are approximated in the Laplace-domain to avoid the above-mentioned drawbacks. Indeed, equations describing the network are represented in a matrix form using the modified nodal admittance (MNA) matrix. Then, it is possible to find the poles of the transfer functions by the well-known Newton's method. Once poles

[1] Present address: Hay Sadri, Rue 10, no 135, Groupe 3, Casablanca, Morocco.

0305-4470/02/337125+11$30.00 © 2002 IOP Publishing Ltd Printed in the UK

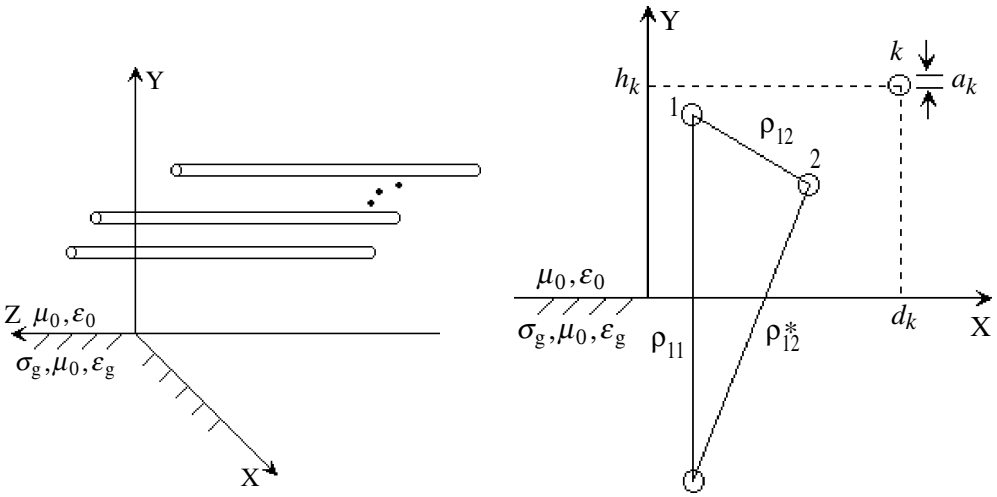

Figure 1. The transmission line geometry.

and residues of transfer functions are obtained, expressions for switching transients may be accomplished in closed form for sine-wave sources.

2. Distributed line parameter model

With the assumption of quasi-TEM wave propagation, the distributions of voltages and currents in an m above-ground coupled transmission-line system can be described by the generalized telegraphist's equations in the frequency s-domain [3, 6]:

$$\frac{\partial \mathbf{V}(z,s)}{\partial z} = -\mathbf{Z}(s)\mathbf{I}(z,s) \tag{1}$$

$$\frac{\partial \mathbf{I}(z,s)}{\partial z} = -\mathbf{Y}(s)\mathbf{V}(z,s) \tag{2}$$

where $0 < z < l$, and $\mathbf{V}(z,s)$ and $\mathbf{I}(z,s)$ are column vectors defining the voltages $v_k(z,s)$ and currents $i_k(z,s)$ distributing along the conductors $k = 1, 2, 3, \ldots, m$. l is the length of the line, $\mathbf{Z}(s)$ and $\mathbf{Y}(s)$ are $m \times m$ dimensional matrices which represent the series impedance and the shunt admittance per unit length of the line, respectively. Figure 1 illustrates the geometry of the line over a ground plane taken as a reference conductor. A series of m parallel wires is located in the air ($y > 0$) above a conducting ground ($y < 0$) with electrical parameters σ_g, ε_g and μ_0. The kth wire has a radius of a_k, and is located at height $y = h_k$ and a position $x = d_k$.

The characteristic parameters, $\mathbf{Z}(s)$ and $\mathbf{Y}(s)$, appearing in the transmission line model of equations (1) and (2), take the following expressions:

$$\mathbf{Z}(s) = \mathbf{Z}_w(s) + s\left(\mathbf{L} + \frac{\mu_0}{2\pi}\mathbf{J}\right) \tag{3}$$

$$\mathbf{Y}(s) = \frac{s}{v^2}\left(\mathbf{L} + \frac{\mu_0}{2\pi}\mathbf{G}\right)^{-1} = \frac{s}{v^2}\left(v^2\mathbf{C}^{-1} + \frac{1}{2\pi\varepsilon_0}\mathbf{G}\right)^{-1} \tag{4}$$

in terms of the inductance matrix $\mathbf{L}$, of the capacitance matrix $\mathbf{C}$, and of the internal impedance matrix of the wires $\mathbf{Z}_w$ with respect to the ground. v is the speed of light in air. The matrix

J represents the conduction losses in the ground. Furthermore, considering the fact that the soil is of finite conductivity, it is also necessary to take into account the displacement current losses in it. Such a contribution is represented by the matrix **G**. Note that the particular case $\sigma_g \to \infty$, that is to say the ground is perfectly conducting, yields $\mathbf{G} = \mathbf{0}$ and $\mathbf{J} = \mathbf{0}$.

The quantities of equations (3) and (4), which are obtained as a consequence of applying the quasi-TEM approximation directly to scattering theory equations, have been detailed in [6]. The result is repeated here.

The elements of the inductance matrix are

$$\mathbf{L}_{kl} = \frac{\mu_0}{2\pi} \ln\left(\frac{\rho^*_{kl}}{\rho_{kl}}\right) \qquad (k, l = 1, 2, \ldots, m) \tag{5}$$

where $\rho_{kl} = \rho_{lk}$ indicates the distance between the centres of the kth and lth wires, which reduces to the radius of the kth wire for $k = l$, and $\rho^*_{kl} = \rho^*_{lk}$ the distance of the ith wire from the image of the kth wire with respect to the air–ground interface.

The capacitance matrix **C** can be expressed in terms of the inductance matrix **L**:

$$\mathbf{C} = v^2 \mathbf{L}^{-1}. \tag{6}$$

The internal impedance matrix elements $\mathbf{Z}_{wkl}$ can easily be determined for various conductor types [8]. For thin solid conductors

$$\begin{aligned} \mathbf{Z}_{wkl} &= \frac{\mu_w}{2\pi b_k} \sqrt{s} \frac{I_0(b_k\sqrt{s})}{I_1(b_k\sqrt{s})} \delta_{kl} \\ \delta_{kl} &= \begin{cases} 1, & k = l \\ 0, & k \neq l \end{cases} \qquad (k, l = 1, 2, \ldots, m) \end{aligned} \tag{7}$$

where $b_k = a_k\sqrt{\sigma_w \mu_w}$, with μ_w and σ_w the electrical parameters characterizing the kth wire. $I_0(z)$ and $I_1(z)$ are the modified Bessel functions.

The contribution of losses in the ground is specified by the matrices **G** and **J** whose elements are [6, 7]

$$\mathbf{J}_{kl} = \int_{-\infty}^{+\infty} \frac{\exp(-|\lambda|\,(h_k + h_l) - \mathrm{i}\lambda\,|d_k - d_l|)}{|\lambda| + \sqrt{\lambda^2 - k_0^2(n^2 - 1)}}\,\mathrm{d}\lambda \tag{8}$$

$$\mathbf{G}_{kl} = \int_{-\infty}^{+\infty} \frac{\exp(-|\lambda|\,(h_k + h_l) - \mathrm{i}\lambda\,|d_k - d_l|)}{n^2\,|\lambda| + \sqrt{\lambda^2 - k_0^2(n^2 - 1)}}\,\mathrm{d}\lambda \tag{9}$$

where $n = \sqrt{\varepsilon_g/\varepsilon_0 + \frac{\sigma_g}{\varepsilon_0 s}}$ is the complex refractive index of the ground. $k_0 = \mathrm{i}s/v$ is the propagation constant in air. Note that the integrals (8) and (9) depend on the electrical parameters of the ground and the geometrical configuration of the line.

When dealing with the integrals (8) and (9), the conventional technique for their evaluation is numerical integration. Because the effective length of the integration interval changes as a function of the above-mentioned parameters, the numerical integration process suffers from the fact that the desired accuracy often requires a large number of interval subdivisions. As a consequence, this technique is time consuming, particularly when repeated evaluations are needed.

To avoid this drawback, we have developed simple and accurate analytical expressions for the integrals (8) and (9) in [7], which are valid for all parameters. Only the final results will be quoted here:

$$\mathbf{J}_{kl} = \ln\left(\frac{\rho^c_{kl}}{\rho^*_{kl}}\right) \qquad (k, l = 1, 2, \ldots, m)$$

where $\rho^c_{kl} = \sqrt{(d_k - d_l)^2 + (h_l + h_k + 2/(k_0\sqrt{1 - n^2}))^2}$.

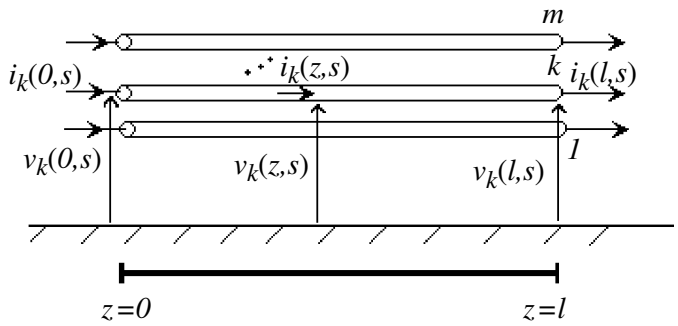

Figure 2. Voltages and currents along the line of length l.

For the elements of the matrix $\mathbf{G}$, some algebraic manipulations are used to rewrite the result from [7] under the following compact form:

$$\mathbf{G}_{kl} = P(\Omega_{kl}) + P(\bar{\Omega}_{kl}) \tag{10}$$

where $\Omega_{kl} = k_0(h_k + h_l + \mathrm{i}|d_k - d_l|)$, $\bar{\Omega}_{kl} = k_0(h_k + h_l - \mathrm{i}|d_k - d_l|)$ and

$$P(z) = \left(-\frac{1}{4} + \frac{1}{2}\frac{1}{n^2+1}\right) Q(bz) + \frac{1}{4} Q\left(bz + \frac{2b}{\sqrt{n^2-1}}\right) - \frac{1}{2}\ln\left(1 + \frac{2}{\sqrt{1-n^2}}\right) \tag{11}$$

with $Q(z) = \exp(-z)\mathbf{E}_1(-z) + \exp(z)\mathbf{E}_1(z)$. The exponential integral is defined by $\mathbf{E}_1(z) = \int_z^\infty \exp(-t)/t \, \mathrm{d}t$ [9, p 228] and $b = \mathrm{i}/\sqrt{n^2+1}$.

3. Formulation of the network equations

In this section, the starting point for determining the network equations is shown in figure 2, which represents an m-wire multiconductor line of length l located over a lossy ground. z represents the length along the line.

The behaviour of the voltages and currents along the line obeys the generalized telegrapher's equations (1) and (2) which can also be written as

$$\frac{\partial \mathbf{\Psi}(z,s)}{\partial z} = -\mathbf{A}(s)\mathbf{\Psi}(z,s) \tag{12}$$

where

$$\mathbf{\Psi}(z,s) = (v_1(z,s), v_2(z,s), \ldots, v_m(z,s), i_1(z,s), i_2(z,s), \ldots, i_m(z,s))^T$$

and

$$\mathbf{A(s)} = \begin{pmatrix} \mathbf{0} & \mathbf{Z}(s) \\ \mathbf{Y}(s) & \mathbf{0} \end{pmatrix}. \tag{13}$$

The general solution for the column vector $\mathbf{\Psi}$ is given by

$$\mathbf{\Psi}(z,s) = \exp(-\mathbf{A}(s)z)\mathbf{\Psi}(0,s) \qquad 0 < z \leqslant l. \tag{14}$$

Superscript T designates the transpose. The matrix exponential $\exp(-\mathbf{A}(s)z)$ and the matrix $\mathbf{A}(s)$ are of dimension $2m \times 2m$.

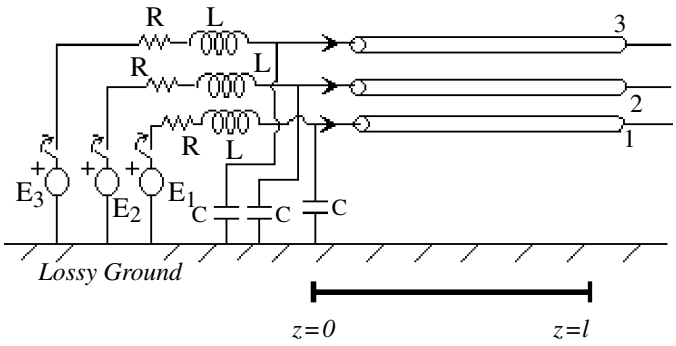

Figure 3. Circuit example for illustrating the formulation. Energization of an open circuited three-phase line.

Let $\mathbf{K}$ designate the matrix exponential $\exp(-\mathbf{A}(s)l)$,

$$\mathbf{K} = \exp(-\mathbf{A}(s)l) = \begin{pmatrix} \mathbf{K}_{1,2} & \mathbf{K}_{1,2} \\ \mathbf{K}_{2,1} & \mathbf{K}_{2,2} \end{pmatrix} \tag{15}$$

where the matrices $\mathbf{K}_{i,j}$ $(i, j = 1, 2)$ are of dimension $m \times m$ and are dependent on s.

Then, it can readily be shown that the terminal currents and voltages at the near end $(z = 0)$ and the far end $(z = l)$ of the line are related by the admittance matrix $\tilde{\mathbf{Y}}$

$$\begin{pmatrix} \mathbf{I}(0, s) \\ -\mathbf{I}(l, s) \end{pmatrix} = \tilde{\mathbf{Y}} \begin{pmatrix} \mathbf{V}(0, s) \\ \mathbf{V}(l, s) \end{pmatrix} = \begin{pmatrix} \tilde{\mathbf{Y}}_{1,1} & \tilde{\mathbf{Y}}_{1,2} \\ \tilde{\mathbf{Y}}_{2,1} & \tilde{\mathbf{Y}}_{2,2} \end{pmatrix} \begin{pmatrix} \mathbf{V}(0, s) \\ \mathbf{V}(l, s) \end{pmatrix} \tag{16}$$

with

$$\tilde{\mathbf{Y}}_{1,1} = \tilde{\mathbf{Y}}_{2,2} = -\mathbf{K}_{1,2}^{-1}\mathbf{K}_{1,1} \qquad \tilde{\mathbf{Y}}_{1,2} = \tilde{\mathbf{Y}}_{2,1} = \mathbf{K}_{1,2}^{-1}. \tag{17}$$

Now, we deal with a simple power system in order to illustrate the formulation. The network configuration consists of an open circuited three-phase line shown in figure 3.

The Laplace transform of Kirchhoff's laws which are applied to the source network leads to

$$(R + Ls)\mathbf{V}(0, s) + (LCs^2 + RCs + 1)\mathbf{I}(0, s) = \mathbf{E}. \tag{18}$$

It should be noted that R and L are scalars. The column vector $\mathbf{E}$ is defined by $\mathbf{E} = (E_1, E_2, E_3)^T$ with E_j $(j = 1, 2, 3)$ the independent sources of the network.

If we combine equations (16) and (18), we may obtain a modified nodal analysis representation of the network

$$\mathbf{y}(s)\boldsymbol{\chi}(s) = \mathbf{e}(s) \tag{19}$$

where the modified nodal admittance matrix $\mathbf{y}(s)$ is given by

$$\mathbf{y}(s) = \begin{pmatrix} \tilde{\mathbf{Y}}_{1,1} & \tilde{\mathbf{Y}}_{1,2} & -\mathbf{U} \\ \tilde{\mathbf{Y}}_{21} & \tilde{\mathbf{Y}}_{2,1} & \mathbf{0} \\ (CLs^2 + RCs + 1)\mathbf{U} & \mathbf{0} & (R + Ls)\mathbf{U} \end{pmatrix}. \tag{20}$$

$\mathbf{U}$ is the unit matrix of dimension 3×3. $\boldsymbol{\chi}(s) = (\mathbf{V}(0, s), \mathbf{V}(l, s), \mathbf{I}(0, s))^T$ is the vector corresponding to the circuit variables.

4. Transfer functions

When one substitutes for the vector $\mathbf{e}(s)$ a constant vector $\mathbf{c}$ with entries determined by the independent sources so that ($c_i \in \{0, 1\}$, $i = 1, 9$), the elements of $\chi(s)$ are called the network transfer functions. The impulse response of the network is the time function $\chi(t)$.

Consider the partial fraction expansion of the network transfer function $\chi(s)$

$$\chi(s) = \sum_{\alpha=1} \frac{\mathbf{r}_\alpha}{s - \lambda_\alpha}. \tag{21}$$

The impulse response $\chi(t)$ is then expressed as a sum of exponential terms

$$\chi(t) = \sum_{\alpha=1} \mathbf{r}_\alpha \exp(\lambda_\alpha t) \tag{22}$$

where λ_α are the poles of $\chi(s)$ and $\mathbf{r}_\alpha$ their associated residues. While replacing $\mathbf{e}(s)$ by $\mathbf{c}$ in (19), one can easily show that λ_α are zeros of $\det(\mathbf{y}(s))$.

In locating the poles in the complex s-plane, the Newton–Raphson algorithm has been adopted. To use such a procedure, the first derivative $\mathbf{y}^{(1)}(s)$ of the network matrix $\mathbf{y}(s)$ with respect to s is needed. This is given by

$$\mathbf{y}^{(1)}(s) = \frac{\mathrm{d}\mathbf{y}(s)}{\mathrm{d}s} = \begin{pmatrix} \tilde{\mathbf{Y}}^{(1)}_{1,1} & \tilde{\mathbf{Y}}^{(1)}_{1,2} & \mathbf{0} \\ \tilde{\mathbf{Y}}^{(1)}_{2,1} & \tilde{\mathbf{Y}}^{(1)}_{2,2} & \mathbf{0} \\ C(2Ls + R)\mathbf{U} & \mathbf{0} & L\mathbf{U} \end{pmatrix}. \tag{23}$$

The superscript $^{(1)}$ in the above matrix designates the derivative with respect to s.

The $(\alpha + 1)$th approximation of the pole $\lambda_{\alpha+1}$ is then obtained from the previous approximation λ_α using the equation

$$\lambda_{\alpha+1} = \lambda_\alpha - \frac{\chi_k(\lambda_\alpha)}{[\mathbf{y}^{-1}(\lambda_\alpha)(\mathbf{y}^{(1)}(\lambda_\alpha)\chi(\lambda_\alpha))]_k} \qquad (\alpha \geqslant 0) \tag{24}$$

with

$$\chi(\lambda_\alpha) = \mathbf{y}^{-1}(\lambda_\alpha)\mathbf{c}.$$

In addition, the subscript k designates the kth element of a $3m$ ($m = 3$) dimensional vector. Since all the network transfer functions have the same poles, k takes an arbitrary fixed value between 1 and $3m$.

After choosing an initial guess λ_0 to the pole, the iteration should be stopped when $\Delta\lambda < \varepsilon$ ($\Delta\lambda = \lambda_{\alpha+1} - \lambda_\alpha$ and ε is the desired accuracy of the pole).

Let λ^* be a pole of $\chi(s)$. It is then easy to show that its corresponding residue $\mathbf{r}^*$ is given by

$$r^*_k = \frac{\chi^2_k(\lambda^*)}{[\mathbf{y}^{-1}(\lambda^*)(\mathbf{y}^{(1)}(\lambda^*)\chi(\lambda^*))]_k} \qquad (k = 1, 2, \ldots, 3m). \tag{25}$$

An examination of the Newton–Raphson formula in equation (24) shows that it is necessary to calculate the matrix $\mathbf{K}$ and the first derivative of the transmission line admittance matrix $\tilde{\mathbf{Y}}$ with respect to s. In dealing with the matrix $\mathbf{K}$, which is a matrix exponential, the usual method for its computation is based on the eigen analysis of matrices [4]. In this case, $\mathbf{K}$ can be expressed in terms of the eigenvalues and eigenvectors of matrix $\mathbf{A}(s)l$. When using such a method, $\mathrm{d}\tilde{\mathbf{Y}}/\mathrm{d}s$ requires the derivatives of the eigenmodes of the line. Due to tedious matrix operation, this method seems to be complicated for evaluating $\mathrm{d}\tilde{\mathbf{Y}}/\mathrm{d}s$.

In this work, the eigenvalues of the matrix $\mathbf{A}(s)l$ are computed using the **QR**-method [11]. The matrix is first balanced and transformed into upper Hessenberg form. The exponential

matrices can then be expressed as a sum of exponential functions with matrix coefficients. To deal with $\mathrm{d}\tilde{\mathbf{Y}}/\mathrm{d}s$, let us consider the relationship (12). Making use of its first derivative with respect to s, we obtain

$$\frac{\partial \boldsymbol{\Psi}^{(1)}(z,s)}{\partial z} + \mathbf{A}(s)\boldsymbol{\Psi}^{(1)}(z,s) = \mathbf{Q}(z,s) \tag{26}$$

where

$$\mathbf{Q}(z,s) = -\frac{\mathrm{d}\mathbf{A}(s)}{\mathrm{d}s}\boldsymbol{\Psi}(z,s). \tag{27}$$

At this stage, it should be pointed out that the derivative of $\mathbf{A}(s)$ can be obtained by formal differentiation of the expressions given in section 2. To do this, we can proceed using, for example, Maple.

From the theory of ordinary differential equations, we can obtain the general solution of (26) in the form

$$\boldsymbol{\Psi}^{(1)}(z,s) = \exp(-\mathbf{A}(s)z)\left[\int_0^z \exp(\mathbf{A}(s)x)\mathbf{Q}(x,s)\,\mathrm{d}x + \boldsymbol{\Psi}^{(1)}(0,s)\right]. \tag{28}$$

By combining equations (14)–(16), (26) and (27), and using the following boundary conditions:

$$\begin{bmatrix}\mathbf{V}(0,s)\\ \mathbf{V}(l,s)\end{bmatrix} = \begin{pmatrix}\mathbf{U} & \mathbf{0}\\ \mathbf{0} & \mathbf{U}\end{pmatrix} \qquad \begin{bmatrix}\mathbf{V}^{(1)}(0,s)\\ \mathbf{V}^{(1)}(l,s)\end{bmatrix} = \begin{pmatrix}\mathbf{0} & \mathbf{0}\\ \mathbf{0} & \mathbf{0}\end{pmatrix}$$

for equations (14) and (26), we get

$$\begin{pmatrix}\mathbf{0} & \mathbf{0}\\ -\tilde{\mathbf{Y}}^{(1)}_{2,1} & -\tilde{\mathbf{Y}}^{(1)}_{2,2}\end{pmatrix} = \mathbf{K}\left(\mathbf{T}\begin{pmatrix}\mathbf{U} & \mathbf{0}\\ \tilde{\mathbf{Y}}_{1,1} & \tilde{\mathbf{Y}}_{1,2}\end{pmatrix} + \begin{pmatrix}\mathbf{0} & \mathbf{0}\\ \tilde{\mathbf{Y}}^{(1)}_{1,1} & \tilde{\mathbf{Y}}^{(1)}_{1,2}\end{pmatrix}\right) \tag{29}$$

where

$$\mathbf{T} = l\int_0^1 \exp(\mathbf{A}lx)\left(-\frac{\mathrm{d}\mathbf{A}}{\mathrm{d}s}\right)\exp(-\mathbf{A}lx)\,\mathrm{d}x. \tag{30}$$

From (29), one may easily compute the first derivative of the line admittance matrix required for Newton iterations. To save computation time, it is convenient to use integration rules of Gauss type for calculating the matrix $\mathbf{T}$. In this work, we have approximated the integral in (30) using the 4-point Gauss–Legendre [10] rule which provides very good results independently of the parameters of the studied structures.

5. Results

To show the efficiency of our method, we will consider two examples. Thereafter, we will assume that each conductor has a radius of $a = 2.5$ mm and the earth is described by the parameters $\sigma_g = 0.01\ \mho/\mathrm{m}$ and $\varepsilon_{rg} = \varepsilon_g/\varepsilon_o = 15$. The source parameters have the following values: $R = 6.5\,\Omega$, $L = 0.034$ H and $C = 0.005\ \mu$F.

Example 1. The configuration shown in figure 4 consists of the energization of an open circuited single phase line. The line was assumed to have a height $h_1 = 15$ m over the earth and a length $l = 150$ km.

It is easy to show that the conventional line voltage and current satisfy the condition

$$\boldsymbol{\Psi}(z,s^*) = \boldsymbol{\Psi}^*(z,s)$$

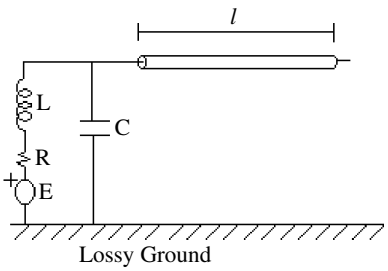

Figure 4. Single-phase line energization.

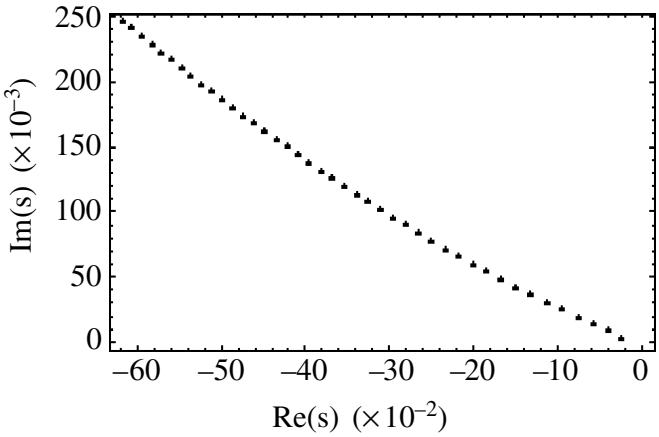

Figure 5. Locations of poles in the upper half plane $\mathrm{Im}(s) > 0$.

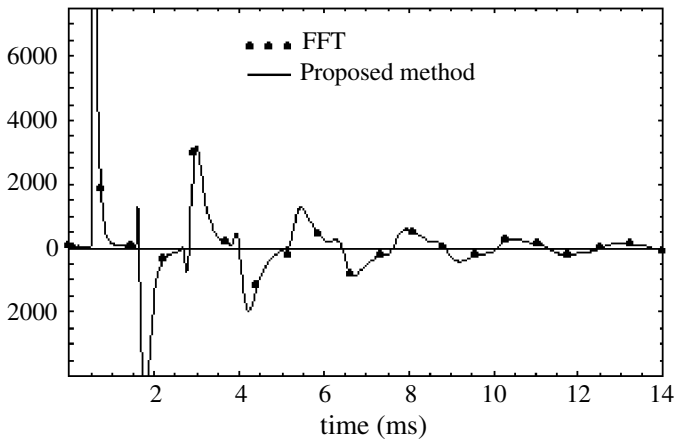

Figure 6. Impulse response at the far end of the line.

where the asterisk denotes the complex conjugate. This property reduces the domain of interest by half. For convenience we use the upper half plane $\mathrm{Im}(s) \geqslant 0$. From this, one immediately infers that the singularities are symmetrically placed with respect to the $\mathrm{Re}(s)$-axis.

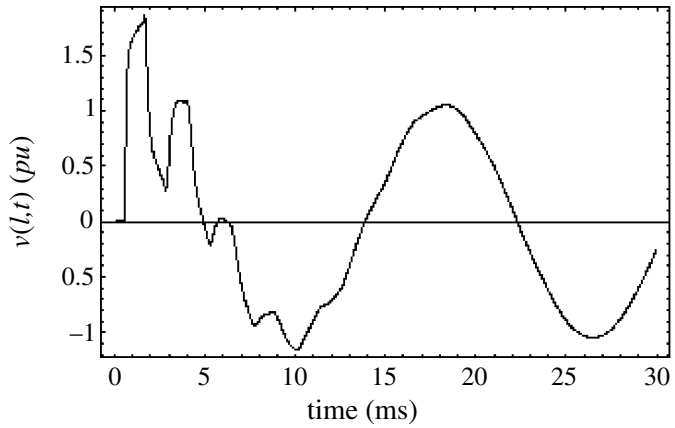

Figure 7. The energizing receiving end response.

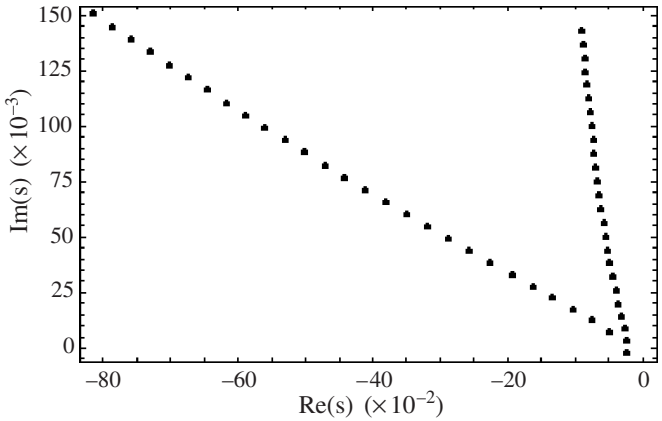

Figure 8. Locations of poles in the upper half plane $\mathrm{Im}(s) > 0$ for three-phase line. In the figure each dot represents a pole.

The poles of the system of figure 4, which occur in complex-conjugate pairs, are obtained using the Newton iterative formula (24). The locations of these poles are depicted in figure 5. It is useful to emphasize here that poles, which are represented by dots in figure 5, are located approximately on a line slightly deviating from the pure imaginary axis ($\mathrm{Im}(s)$-axis). Moreover, the poles are quasiuniformly spaced. It should be noted that the alignment of the poles and the uniformity of the space between them are characteristics that one recovers for all the line parameters. This aspect is a great advantage of our method. Indeed, if we consider two consecutive poles λ_k and λ_{k+1}, which could be reached using starting points on the $\mathrm{Im}(s)$-axis in the s-plane and arranged as $|\lambda_k| < |\lambda_{k+1}|$, we may approximate the complex step between the poles by $\Delta \approx \lambda_{k+1} - \lambda_k$. Then, it is possible to speed up the convergence of the Newton iterative process using starting points λ_α ($\alpha = 1, \ldots, N$) chosen so that $\mathrm{Im}(\lambda_\alpha) = \mathrm{Im}(\lambda_k) + \frac{\mathrm{Im}(\Delta)}{\mathrm{Re}(\Delta)}(\mathrm{Re}(\lambda_\alpha) - \mathrm{Re}(\lambda_k))$. N is the number of required poles.

The transient response $v(l, t)$ at the far end, which is kept open, to the impulse input is computed by using the proposed method and the FFT. The results from the FFT method are obtained from (19) by substituting s for $\mathrm{i}\omega$ and then applying the numerical inverse Fourier

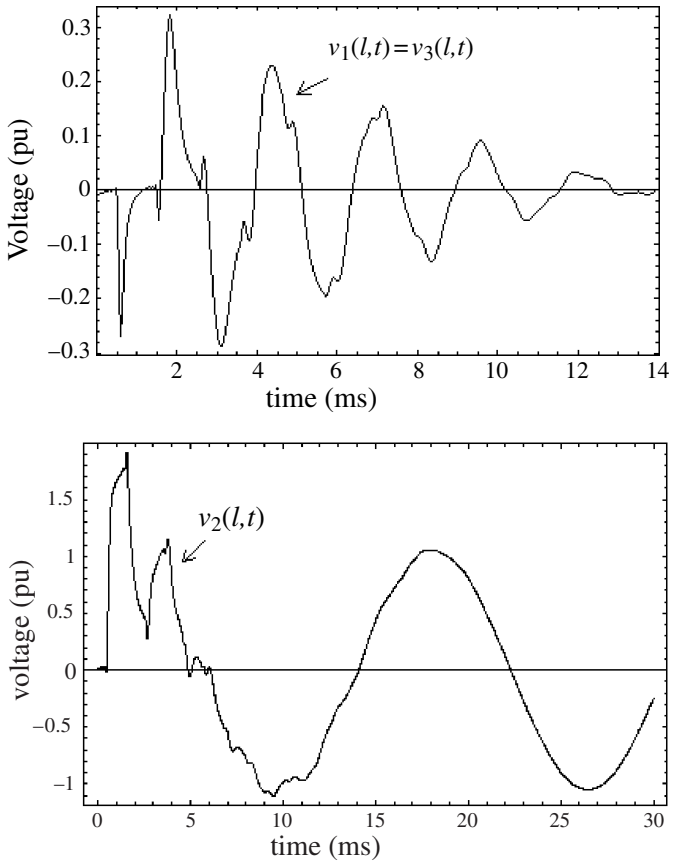

Figure 9. Voltages at receiving three-phase line end.

transform to go from the frequency domain back to the time domain. As shown in figure 6, the results are superimposed. On a Pentium III/1 GHz processor, the FFT method takes 62.01 s to finish this example for 512 harmonics while our method uses only 19.86 s for 15 poles, which is about three times faster. The computation time depends on the number of the poles to be located. Generally, the model incorporating the first four pairs of complex-conjugate poles (dominant poles) is an excellent approximation of the exact transfer functions. Such a model yields substantial computation economies. Furthermore, the amount of computer storage needed is much less than the Fourier requirement. For example, the FFT method requires 70.2 kB for the solution given in figure 6 while the proposed method requires only 45.7 kB. This requirement depends on the number of poles and the total solution times.

The line was energized by a sine-wave source. The Laplace transform of a 60 Hz sinusoidal signal

$$e(t) = U_M \sin(\omega_o t + \phi_o) \tag{31}$$

applied to the line sending end is given by

$$E(s) = U_M \frac{\cos(\phi_o)\omega_o + \sin(\phi_o)s}{s^2 + \omega_o^2}. \tag{32}$$

From (32) and (22), one can easily obtain the line far end voltage in the following closed form:

$$v(l,t) = 2U_M \,\mathrm{Re}\left(r_{2\alpha} \sum_{\alpha} \frac{-\lambda_\alpha \sin(\omega_o t + \phi_o) - \omega_o \cos(\omega_o t + \phi_o)}{\omega_o^2 + \lambda_\alpha^2} + \frac{(\omega_o \cos(\phi_o) + \lambda_\alpha \sin(\phi_o)) \exp(\lambda_\alpha t)}{\omega_o^2 + \lambda_\alpha^2} \right). \tag{33}$$

Figure 7 shows the curve associated with the expression (33) for $\phi_o = \pi/3$.

Example 2. The circuit is shown in figure 3, where three coupled lines are presented. As an example, the geometric parameters of this configuration of lines are assumed to have the following values: $d_{12} = d_{23} = d_{13} = 1$ m, $h_1 = h_3 = 10$ m and $h_2 = 15$ m.

The conductor of height h_2 is excited by the sine-wave source given in (31). The length of the three-conductor line is 150 km. The locations of poles in the complex s-plane are shown in figure 8. The output waveforms at the far end of the line for the simultaneous closing of the switches are drawn in figure 9.

6. Conclusion

An efficient and accurate method for assessing the switching transients in overhead lines is presented. It is based on the formulation of the transmission line network equations in the complex s-domain. The rational approximation of the transfer functions can be easily obtained by locating their poles in the complex s-plane. This is done by using an iterative technique based on Newton's scheme. A simple formula for calculating residues is used. The proposed method permits the calculation of the switching transients in closed-form for sine-wave source.

References

[1] Carson J R 1926 Wave propagation in overhead wires with ground return *Bell Syst. Tech. J.* **5** 539–54

[2] Marti J R 1986 Accurate modeling of frequency-dependent transmission lines in electromagnetic transient simulations *IEEE Trans. Power Appar. Syst.* **1** 147–55

[3] Zeddam A, Koné I, Deguauque P and Demoulin B 1988 Voltages induced on coaxial cables or multi-wire shielded lines by a disturbing wave *Electromagnetics* **8** 311–33

[4] Paul C R 1976 Frequency response of multi-conductor transmission lines illuminated by an electromagnetic field *IEEE Trans. Electromagn. Compat.* **18** 183–90

[5] Plate S W, Chang D C and Kuester E F 1977 Characteristic of discrete propagation modes on a system of horizontal wires over a dissipative earth *Sci. Rept* No 24 (RADC-TR-77-81) Department of Electrical Engineering, University of Colorado, Boulder

[6] Bridges G E, Aboul-Atta O and Shafai L 1988 Solution of discrete modes for wave propagation along multiple conductor structures above a dissipative Earth *Can. J. Phys.* **66** 428–38

[7] Maaouni A, Amri A and Zouhir A 2001 Simple and accurate analytical expressions for evaluating related transmission line integrals *J. Phys. A: Math. Gen.* **34** 9027–35

[8] Vance E F 1978 *Coupling to Shielded Cables* (New York: Wiley–Interscience)

[9] Abramowitz M and Stegun I 1964 *Handbook of Mathematical Functions* (Washington, DC: National Bureau of Standards)

[10] Davis P J and Rabinowitz P 1984 *Methods of Numerical Integration* (New York: Academic)

[11] Press W H, Flannery B P, Teukolsky S A and Vetterling W T 1991 *Numerical Recipes in C: The Art of Scientific Computing* (Cambridge: Cambridge University Press)